ACS SENSORS

Article

Cite This: ACS Sens. XXXX, XXX, XXX−XXX

pubs.acs.org/acssensors

Electrochemical DNA Biosensing via Electrochemically Controlled Reversible Addition−Fragmentation Chain Transfer Polymerization

Qiong Hu,[†,‡] Jinming Kong,[*,†] Dongxue Han,[‡] Li Niu,[*,‡] and Xueji Zhang[*,§]

[†]School of Environmental and Biological Engineering, Nanjing University of Science and Technology, Nanjing 210094, People's Republic of China

[‡]Center for Advanced Analytical Science, School of Chemistry and Chemical Engineering, School of Civil Engineering, Guangzhou University, Guangzhou 510006, People's Republic of China

[§]Beijing Key Laboratory for Bioengineering and Sensing Technology, School of Chemistry and Biological Engineering, University of Science and Technology Beijing, Beijing 100083, People's Republic of China

Supporting Information

ABSTRACT: Sensitive and selective sensing of biological molecules is fundamental to disease diagnosis and infectious disease surveillance. Herein, an ultrasensitive and highly selective electrochemical DNA biosensor is described by exploiting the electrochemically controlled reversible addition−fragmentation chain-transfer (eRAFT) polymerization as a signal amplification strategy and the peptide nucleic acid (PNA) probes as the recognition elements. Specifically, the PNA probes with a thiol at their 5′-terminals are anchored to a gold electrode surface (via gold−sulfur self-assembly) for sequence-specific recognition of target DNA (tDNA) fragments, of which the phosphate sites serve as the anchorages for the targeted labeling (via the well-established phosphate−Zr^{4+}−carboxylate chemistry) of the carboxyl-group-containing chain-transfer agents (CTAs) for the succedent eRAFT polymerization, wherein the initiating radicals are generated through electrochemical reduction of aryl diazonium salts under a potentiostatic condition. In the presence of ferrocenylmethyl methacrylate ($FcCH{=}CH_2$) as the monomer, the grafting of polymer chains from the CTA-anchored sites as a result of the eRAFT polymerization brings numerous electroactive Fc tags to the electrode surface, outputting a high electrochemical sensing signal even in the presence of trace amounts of tDNA fragments. Under the optimized conditions, the linear range of the described electrochemical DNA biosensor spans from 10 aM to 10 pM (R^2 = 0.998), with an attomolar detection limit (4.1 aM) being achieved. Moreover, the described electrochemical DNA biosensor is highly selective and applicable to the sensing of tDNA fragments in complex serum samples. Given its high efficiency, easy operation, and low cost, this biosensor shows great promise in real applications.

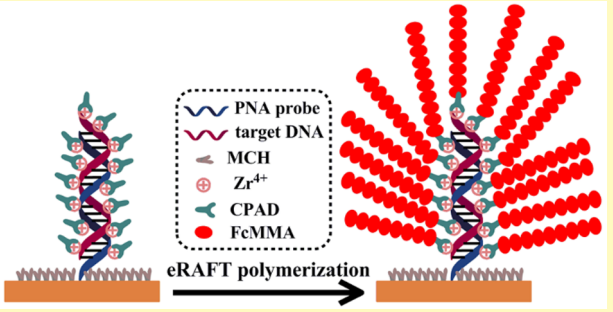

KEYWORDS: *electrochemical, DNA biosensor, reversible addition−fragmentation chain-transfer polymerization, electrochemically controlled radical polymerization, peptide nucleic acid, signal amplification*

As an important research hotspot in biosensing, the highly sensitive and selective sensing of proteins, nucleic acids, and other biological molecules has found broad applications in many fields (e.g., disease diagnosis and infectious disease surveillance).[1] Given the excellent specificity of biorecognition processes, especially for the antigen−antibody interactions and nucleic acid hybridizations, the selectivity of most biosensors is generally very high. In this context, ever-increasing attention has currently been paid to improving the sensing sensitivity of biosensors.

To improve the sensing sensitivity, many strategies have so far been proposed for the amplification of the output signal.[2−6] Taking the electrochemical DNA biosensing (it shows the advantages such as high sensitivity, easy operation, low cost, and rapid response relative to other sensing methods) as an example, the sensing signal can be effectively amplified by using catalytic labels (e.g., natural enzymes,[7] biomimetic catalysts,[8] and electrocatalysts,[9]), metal nanoparticles,[10] or polymers.[11−13] Among them, the polymer-based signal amplification strategies are very impressive. Through the use of polymers, a large number of electroactive tags (e.g., methylene blue (MB)) or functional sites (e.g., $-NH_2$ and -COOH) that are available for the further conjugation of electroactive tags can be introduced, thereby substantially amplifying the electrochemical sensing signal.[12,14,15] The polymer-based strategies can be categorized into the "grafting-to" and "grafting-from" subclasses. The grafting-to strategies are based on the use of ready-made polymers. Examples include the use of the oligonucleotide fragments (as the auxiliary

Received: November 4, 2018
Accepted: December 25, 2018

DOI: 10.1021/acssensors.8b01357
ACS Sens. XXXX, XXX, XXX−XXX

detection probe) and block copolymers containing ferrocene (Fc) side chains by Gibbs et al.[16] and the Fc-conjugated cationic polythiophene by Le Floch et al.[13] for the electrochemical biosensing of DNA, in which the block copolymers or the positively charged polymers can be directly grafted to the electrode surface by means of sandwich hybridization reaction or electrostatic adsorption, respectively. Although the grafting-to strategies are relatively easy in operation, they suffer from the drawback of sluggish grafting kinetics since the loss in conformational entropy of the randomly coiled chains significantly suppresses the polymers from diffusing to and eventually reacting with the binding sites.[17−19] To address this issue, the grafting-from strategies, i.e., ab initio polymerization, seem to be ideal solutions of choice. Using deoxyribonucleotide triphosphates (dNTPs, N = A, T, G, or C) as the monomers, for example, the grafting of long oligonucleotide fragments from the electrode surface, mediated by the rolling circle amplification (RCA)[20] or catalyzed by the terminal deoxynucleotidyl transferase (TdT),[21] can provide numerous negatively charged phosphate sites for the electrostatic adsorption of positively charged electroactive tags (e.g., $[Ru(NH_3)_6]^{3+}$), thereby substantially amplifying the electrochemical sensing signal. Nevertheless, the presence of oligonucleotide fragments as the recognition probes can also lead to the electrostatic adsorption of electroactive tags, producing a very high background signal. Furthermore, these two strategies require the use of natural enzymes (e.g., phi29 DNA polymerase or TdT), suffering from the drawbacks of high cost and stringent reaction conditions. Alternatively, using oligonucleotide fragments as the monomers, the grafted products of the catalytic hairpin assembly (CHA),[22] the hybridization chain reaction (HCR),[23] or the supersandwich hybridization reaction (SSHR)[24] are long double-stranded DNA (dsDNA) fragments, through which numerous electroactive tags can also be introduced. However, the use of oligonucleotide fragments as the monomers suffers from the defects of high cost and insufficient hybridization efficiency, whereas the electrostatic adsorption of the electroactive tags (e.g., $[Ru(NH_3)_6]^{3+}$) to the recognition probes can also raise the background electrochemical signal.

To overcome the above drawbacks, the reversible deactivation controlled/"living" radical polymerization (RDRP) methods such as the atom-transfer radical polymerization (ATRP) have been incorporated into the electrochemical biosensing of DNA. For example, Wu et al. and our group have successfully demonstrated the potential use of the activators generated electron transfer (AGET) for ATRP (AGET ATRP)[25] and the electrochemically controlled ATRP (eATRP)[18] for the electrochemical biosensing of DNA. Through the ATRP, a high density of polymer chains containing numerous electroactive tags can be grafted from the initiator-anchored electrode surface, causing a substantial amplification of the electrochemical sensing signal.[18] Relative to the use of dNTPs or oligonucleotide fragments as the monomers, the ATRP-mediated ab initio polymerization features the merits of high efficiency, easy operation, and low cost.[18,26] However, ATRP involves the use of transition metal complexes (e.g., Cu^{I}/L and $Cu^{II}Br/L$; L = ligand) as the activators and deactivators,[27] of which the toxicity raises considerable concerns for further biomedical applications; in particular, the metal residues are found to interfere with the final electrochemical tests.[12,28]

In 1998, the CSIRO group from Australia reported an another RDRP technique named reversible addition−fragmentation chain-transfer (RAFT) polymerization,[29] which operates through the principle of degenerative chain transfer (also termed reversible chain transfer), with thiocarbonylthio compounds (S═C(Z)S−R, e.g., dithiobenzoates, dithioesters, or trithiocarbonates) as the chain-transfer agents (CTAs).[29−31] Of the RAFT polymerization, the living character stems from the reversible transfer of the S═C(Z)S- moiety between the propagating radicals and the dormant chains.[29,32] Given its merits such as broad availability of vinyl monomers (e.g., (meth)acrylamides, (meth)acrylates, and even acrylic acid), mild reaction conditions (from the viewpoint of industrial production), good compatibility with various polymerization systems (e.g., bulk, solution, emulsion, and suspension), and high reaction orthogonality,[33,34] RAFT polymerization has been intensively investigated in the synthesis of various polymers with desired molecular weights, high end-group fidelity, controlled architectures, and narrow dispersity.[31,35,36] Particularly impressive is the absence of transition metal complexes, which makes the RAFT polymerization biologically friendly. With these in mind, we have lately reported a RAFT polymerization-based electrochemical DNA biosensor, through which the target DNA fragments with an attomolar concentration (as low as 3.2 aM) has been sensitively sensed.[12] In the RAFT polymerization, the initiating radicals are generally generated through thermal decomposition of azo radical initiators (e.g., 2,2′-azobis(2,4-dimethyl)valeronitrile (ABVN) and azodiisobutyronitrile (AIBN)) between 50 and 70 °C.[31] Although relatively simple in operation, such a high initiation temperature may cause the denaturation and/or deactivation of thermolabile biological molecules such as DNA/DNA duplexes and enzymes. Furthermore, some thiocarbonylthio compounds are also thermally unstable; for example, the water-soluble 4-cyano-4-(phenylcarbonothioylthio)pentanoic acid (CPAD) can be decomposed by ∼36% at 50 °C and by ∼84% at 60 °C, after a period of 24 h.[37] For these reasons, the generation of initiating radicals under mild conditions is highly desired. Recently, Matyjaszewski's group reported the electrochemically controlled RAFT polymerization, i.e., eRAFT polymerization, of which the initiating radicals were generated through electrochemical reduction of 4-bromobenzenediazonium tetrafluoroborate ($BrPhN_2^+$) or benzoyl peroxide (BPO) at room temperature.[38] Through the eRAFT polymerization, well-defined polymers with desired molecular weight and narrow dispersity have been successfully synthesized. Nevertheless, the eRAFT polymerization has not yet been incorporated into the electrochemical biosensing of DNA, to our knowledge.

Herein, we describe an ultrasensitive and highly selective electrochemical DNA biosensor, by exploiting the eRAFT polymerization as a signal amplification strategy together with the utilization of the peptide nucleic acid (PNA) probes as the sequence-specific recognition elements. PNA—a oligonucleotide analogue synthesized by replacing the negatively charged (deoxy)ribose phosphate backbone of oligonucleotides with the uncharged peptide backbone[39]—is utilized as the recognition element for the sequence-specific capture of target DNA (tDNA) fragments, by virtue of its superb discrimination capability toward single-base mismatch.[39−41] After the targeted labeling of the carboxyl-group-containing dithiobenzoates (as the CTAs) to the captured tDNA fragments and the succedent eRAFT polymerization using $FcCH{=}CH_2$ as the vinyl

DOI: 10.1021/acssensors.8b01357
ACS Sens. XXXX, XXX, XXX−XXX

monomer, a high density of polymers containing numerous electroactive Fc tags can be grafted from the electrode surface, consequently substantially amplifying the sensing signal. Under the optimized conditions, a good logarithmic relationship between the sensing signal and the tDNA-fragment concentration over 7 orders of magnitude spanning from 10 aM to 10 pM (R^2 = 0.998), with a limit of detection (LOD) down to the attomolar level (4.1 aM), can be achieved. In addition, results show that the described electrochemical DNA biosensor is applicable to genotyping of single-nucleotide polymorphisms (SNPs) as well as to the detection of tDNA fragments in complex serum samples. Furthermore, the described electrochemical DNA biosensor features the merits of high efficiency, easy operation, and low cost. Taking these into consideration, the combined use of the eRAFT polymerization as the signal amplification strategy and the PNA probes as the recognition elements shows great promise in the ultrasensitive and highly selective electrochemical DNA biosensing.

EXPERIMENTAL SECTION

Materials and Reagents. PNA probe with a thiol at the 5′-terminal was tailor-made and purified by CP Biochem Co., Ltd. (Chengdu, China). Four oligonucleotide fragments, including the tDNA fragment, the ones with a single-base (SBM) or three-base (TBM) mismatch, and the control one (cDNA), were all synthesized and purified (HPLC) by Sangon Biotech (Shanghai, China). The sequences of the PNA probe and the four oligonucleotide fragments (with mismatch(es) underlined) are presented in Supporting Information Table S1.

6-Mercapto-1-hexanol (MCH), tetrabutylammonium perchlorate (TBAP), $LiClO_4$, $ZrOCl_2$, and KPF_6 were all provided by J&K Scientific Ltd. (Shanghai, China). CPAD, $BrPhN_2^+$, normal human serum (NHS), and $FcCH{=}CH_2$ were supplied by Aladdin Bio-Chem Technology Co., Ltd. (Shanghai, China), Tokyo Chemical Industry (Shanghai, China), YiJi Industrial Co., Ltd. (Shanghai, China), and Sigma-Aldrich (St. Louis, MO, USA), respectively. All chemicals such as absolute ethanol (EtOH) and *N*,*N*-dimethylformamide (DMF) were of analytical purity and used directly as supplied. Ultrapure water (upH_2O, ≥ 18.25 MΩ cm) was purified by a Millipore Milli-Q purification system.

The solutions of PNA probe, MCH, oligonucleotide fragments, $ZrOCl_2$, CPAD, $FcCH{=}CH_2$, and $BrPhN_2^+$ were prepared with upH_2O, 60% EtOH, 0.1 M phosphate-buffered solution (PBS, pH 7.4), 15% EtOH, 15% EtOH, DMF, and DMF, respectively. The eRAFT polymerization solution was prepared prior to each use by sequentially adding 0.1 mL of 0.01 M $FcCH{=}CH_2$, 5 μL of 0.01 M $BrPhN_2^+$, and 8 mL of 0.1 M KPF_6 into 1.895 mL of DMF.

Apparatus. Electrochemical impedance spectroscopy (EIS) was tested in 5 mM $[Fe(CN)_6]^{4-/3-}$ (prepared with 0.1 M KNO_3), using an Autolab/PGSTAT302N galvanostat/potentiostat (Eco Chemie); the open circuit potential, the amplitude of sine wave potential, and the frequency range were 0.18 V, 5 mV, and 100 kHz to 0.1 Hz, respectively. Other electrochemical tests were conducted with a CHI 760D electrochemical workstation (CH Instruments Inc.). Electrochemical tests were all carried out at room temperature, using a platinum wire (Pt) auxiliary electrode, a gold (AuE, Φ = 2 mm) working electrode, and a saturated calomel (SCE) reference electrode. The micrographs were collected with a field emission scanning electron microscope (SEM, Quanta 250F, FEI) at an accelerating voltage of 30 kV.

Electrochemical Biosensing of DNA. The AuE surface was carefully polished before each use to mirror-like finish with Al_2O_3 slurries (0.3 and 0.05 μm in sequence), sonicated in EtOH and upH_2O, soaked for 15 min in "piranha solution" (a mixture of 30% H_2O_2 and 98% H_2SO_4 (1:3, v/v); ***Caution!*** *The mixture is highly corrosive*), and then rinsed with upH_2O. Following this, the AuE surface was treated by cyclic voltammetry (CV) at a scan rate of 0.1 V s^{-1} (initial potential, − 0.3 V; high potential, 1.5 V; low/final potential, − 0.3 V) in 0.5 M H_2SO_4, until a reproducible CV curve was observed.[12] After soaking (15 min) in $NaBH_4$ solution, it was sonicated in upH_2O and dried with N_2.

A 5 μL aliquot of 0.5 μM PNA probe was dropped onto the AuE surface, which was then incubated (1 h) and thoroughly rinsed with upH_2O. The AuE surface was then blocked by MCH (2 mM) and rinsed with EtOH and upH_2O. Onto the AuE surface, 10 μL of tDNA fragments was added, followed by incubation (1.5 h) and gentle rinsing with 0.1 M PBS. After that, it was soaked in 5 mM Zr^{4+} for 15 min and rinsed with upH_2O. After soaking (0.5 h) in 0.5 mM CPAD, it was rinsed with 15% EtOH and upH_2O. Afterward, the modified AuE was soaked in the eRAFT polymerization solution (stirred vigorously to suppress the grafting of initiating radicals onto the AuE surface), followed by the eRAFT polymerization (1.5 h) at room temperature under a potentiostatic condition (using *i*−*t* curve). Unless otherwise specified, the sequential modification of the AuE surface mentioned above was performed at 37 °C. After the eRAFT polymerization, the AuE surface was successively rinsed with DMF and upH_2O, and measured in 0.5 M $LiClO_4$ solution by square wave voltammetry (SWV; quiet time, 30 s; increase potential, 4 mV; frequency, 15 Hz; potential amplitude, 0.025 V).

RESULTS AND DISCUSSION

Principle of the Described Electrochemical DNA Biosensor. Scheme 1 presents the sensing principle of the described electrochemical DNA biosensor. PNA is used here as the recognition element for the sequence-specific capture of tDNA fragments by virtue of its superb specificity.[40] Importantly, the backbone of the PNA molecule is composed of the neutral *N*-(2-aminoethyl)glycine (AEG) component. Thus, the hybridization of the tDNA fragments to the PNA elements can bring the phosphate sites to the electrode surface, which can then be taken advantage of as the anchorages for the targeted labeling of the carboxyl-group-containing CTAs, e.g., CPAD, via the well-established phosphate−Zr^{4+}−carboxylate chemistry which has found a broad application in surface functionalization due to the strong ionic and coordinative interactions between Zr^{4+} ions and the phosphate groups and carboxylate groups.[18,42] Subsequently, electrochemical reduction of the diazonium salt $BrPhN_2^+$ produces the highly reactive aryl radicals,[43] which can serve as the initiating radicals for the eRAFT polymerization.[38] Through the eRAFT polymerization with $FcCH{=}CH_2$ as the monomer, dense polymers containing numerous electroactive Fc tags can be

Scheme 1. Schematic Illustration of the eRAFT Polymerization-Based Electrochemical DNA Biosensor

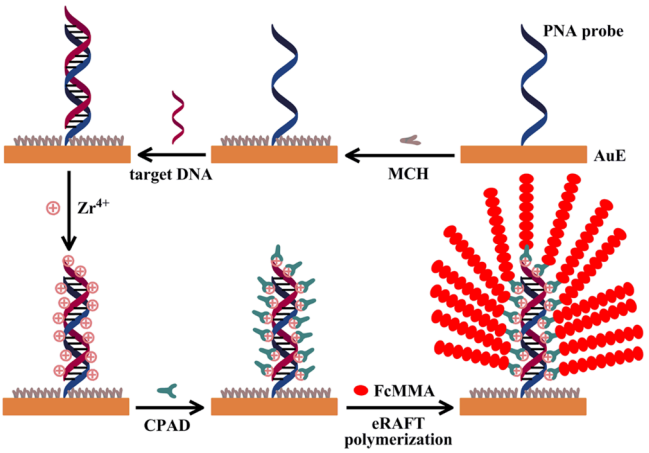

DOI: 10.1021/acssensors.8b01357
ACS Sens. XXXX, XXX, XXX−XXX

grafted from the AuE surface, causing a substantial amplification of the electrochemical sensing signal. Thus, the combined use of the eRAFT polymerization as a signal amplification strategy and the PNA probes as the recognition elements allows the ultrasensitive and highly sensitive sensing of tDNA fragments. In the surface grafting, the CTAs can be anchored to the phosphate sites via either the Z group or the R group.[44] However, the grafting of polymer chains with anchoring of the R group of the CTAs offers benefits relative to that with the Z group.[44] In the latter case, the anchored thiocarbonylthio moiety may be less and less accessible with the growth of polymer chains, considering that the chain-transfer reaction between the anchored CTAs and the free polymeric radicals takes place close to the AuE surface.[44,45] That is, the latter case suffers from a lower grafting density of polymer chains caused by the shielding effect.[44,46] In contrast, the former case allows the grafting of a relatively higher density of polymer chains with higher molecular weight,[44,45] which undoubtedly favors the signal amplification in consideration of the introduction of many more Fc tags.

Electrochemical Properties of CPAD and $BrPhN_2^+$. Through electrochemical reduction, the weak C−S bond of CPAD can be irreversibly cleaved, generating two anionic fragments.[38] Therefore, it is necessary to make it clear that the molecular structure of CPAD is not decomposed during the electrochemical reduction of $BrPhN_2^+$. Using a glassy carbon working electrode (GCE, Φ = 3 mm), the electrochemical properties of CPAD and $BrPhN_2^+$ were studied by CV in 0.1 M TBAP (prepared with DMF, N_2 saturated). The cyclic voltammograms are shown in Figure 1A. The voltammogram

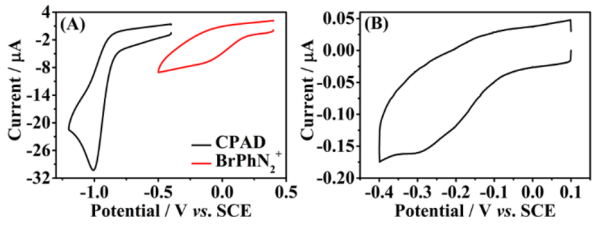

Figure 1. (A) Cyclic voltammograms (CVs) of 1 mM CPAD and 1 mM $BrPhN_2^+$ in 0.1 M TBAP (N_2 saturated) and (B) those of the PNA/MCH/tDNA/Zr^{4+}/CPAD-modified AuE in the FcCH═CH_2-free eRAFT polymerization solution. The concentration of tDNA fragment was 10 pM.

of CPAD shows an irreversible reduction peak at −1 V, which is in agreement with the reported value.[38] Of $BrPhN_2^+$, the irreversible reduction peak is located at the potential of −0.1 V, being 0.9 V more positive than that of the CPAD. Since the reduction waves of CPAD and $BrPhN_2^+$ do not overlap with each other, the initiating radicals of the eRAFT polymerization can be generated through electrochemical reduction of $BrPhN_2^+$.

Potential of the eRAFT Polymerization. Using the PNA/MCH/tDNA/Zr^{4+}/CPAD-modified AuE as the working electrode, the potential window applicable for the electrogeneration of the initiating radicals was interrogated by CV in the FcCH═CH_2-free eRAFT polymerization solution.[47] As shown in Figure 1B, the voltammogram presents an irreversible reduction peak at −0.3 V, which corresponds to the generation of initiating radicals at the AuE surface. The initiating radicals are quite reactive that can readily graft onto the AuE surface.[42] To suppress the surface grafting of initiating radicals, a relatively positive reduction potential should therefore be applied. However, this may result in a slower polymerization rate due to the generation of a lower concentration of the initiating radicals. Therefore, the eRAFT polymerization was conducted at −0.3 V. Figure S1 shows a typical $i-t$ curve of the eRAFT polymerization; the total charge consumed during the polymerization (~1.5 mC) that corresponds to the electrochemical reduction of $BrPhN_2^+$ can be correlated to the grafting amount of polymer chains from the AuE surface.

Characterizations. The feasibility of the eRAFT polymerization-based biosensor was studied by SWV. As observed from Figure 2A(a), a strong oxidation peak representing the

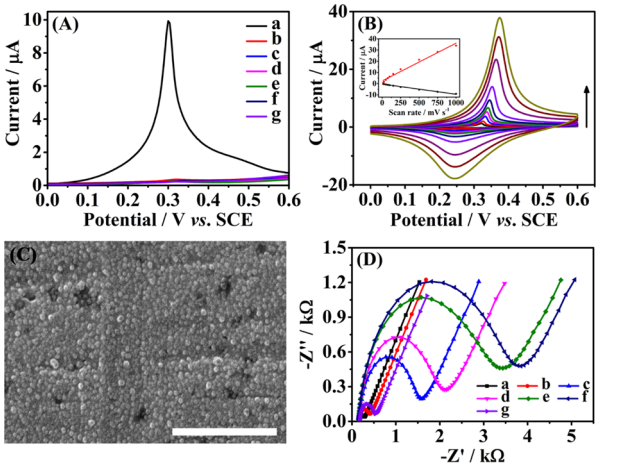

Figure 2. (A) Square wave voltammograms (SWVs) of the as-modified AuE (a) and of those modified without PNA probes (b), tDNA fragments (c), Zr^{4+} linkers (d), CPAD (e), $BrPhN_2^+$ (f), or FcCH═CH_2 (g). (B) Scan-rate-dependent CVs of the polymer-grafted AuE. Along the arrow, the scan rate was varied from 10 to 1000 mV s^{-1}. Inset presents the correlation of the anodic (marked red) and cathodic (marked black) peak currents with the scan rate. (C) SEM image of the polymer-grafted AuE. The scale bar is 1 μm. (D) Nyquist plots of the bare AuE (a) and of those obtained after the sequential modification of PNA (b), MCH (c), tDNA fragments (d), Zr^{4+} linkers (e), CPAD (f), and Fc tags (g). The concentration of tDNA fragment was 10 pM.

electrochemical oxidation of Fc tags appears at the potential of ~0.3 V,[12] in case the electrochemical DNA biosensor was prepared as described. Otherwise, no observable oxidation peak appears if it was prepared without PNA probes (Figure 2A(b)), tDNA fragments (Figure 2A(c)), Zr^{4+} linkers (Figure 2A(d), CPAD (Figure 2A(e)), $BrPhN_2^+$ (Figure 2A(f)), or FcCH═CH_2 (Figure 2A(g)). These results validate the feasibility of the described electrochemical DNA biosensor. Further, the redox properties of the grafted polymers were studied by CV. Figure 2B shows the scan-rate-dependent voltammograms. As observed, the redox currents are linearly related to the scan rate (inset in Figure 2B), demonstrating that the polymers are tied to the AuE surface.[12,19]

After the eRAFT polymerization, the surface morphology of the AuE was observed with SEM. As observed from Figure 2C, dense polymer particles are stacked on the AuE surface, signifying the high efficiency of the eRAFT polymerization. Furthermore, the dense traces of the P (Figure S2A) and Fe elements (Figure S2B), as tracked by EDS (energy-dispersive X-ray spectroscopy), represent the presence of the tDNA fragments and especially a very large number of Fc tags.[12,18]

DOI: 10.1021/acssensors.8b01357
ACS Sens. XXXX, XXX, XXX−XXX

Further, the preparation of the eRAFT polymerization-based biosensor was characterized by EIS, of which the Nyquist plots are presented in Figure 2D. As observed, the bare AuE shows a relatively small charge-transfer resistance (R_{ct} ~ 0.14 kΩ; Figure 2D(a)). The self-assembly of the PNA probe layer (~0.26 kΩ; Figure 2D(b)) and the MCH layer (~1.39 kΩ; Figure 2D(c)) can raise the R_{ct}, which is caused by the steric hindrance from the PNA or PNA/MCH monolayer.[18] Further increase in the R_{ct} is observed after the hybridization of the tDNA fragments to the PNA probes (~1.91 kΩ; Figure 2D(d)), owing to the synergic effect of the electrostatic repulsion and the steric hindrance of the negatively charged tDNA fragments.[12,18] The coordination of Zr^{4+} linkers to the phosphate sites raises the R_{ct} (~3.11 kΩ; Figure 2D(e)), due to the presence of the electrostatic repulsion from the preadsorbed $[Fe(CN)_6]^{4-/3-}$ to the incoming ones.[18,19] Also, the targeted labeling of CPAD causes a further increase in the R_{ct} (~3.68 kΩ; Figure 2D(f)), as $[Fe(CN)_6]^{4-/3-}$ is ejected from the AuE surface caused by the decrease of surface hydrophilicity.[12,18] Last, the eRAFT polymerization leads to a drastic decrease in R_{ct} (~0.47 kΩ; Figure 2D(g)), which is caused by the grafting of dense electroactive polymers.[12] The obtained results validate the successful preparation of the eRAFT polymerization-based biosensor.

Optimization of $BrPhN_2^+$ Concentration. Electrochemical reduction of the diazonium salt $BrPhN_2^+$ produces the aryl radicals, which not only can act as the initiating radicals for the eRAFT polymerization but also can graft to the AuE surface. Since the presence of an insulating aryl layer can dissipate the applied voltage,[38] a higher $BrPhN_2^+$ concentration is believed to be detrimental to the eRAFT polymerization. On the other hand, a slower polymerization rate will be suffered if the concentration of the initiating radicals is too low.[12] Thus, the concentration of $BrPhN_2^+$ should be optimized. As observed from Figure S3, the sensing signal at ~0.3 V increases with the increase of $BrPhN_2^+$ concentration from 1 to 5 μM; after that, it decreases significantly with the further increase of $BrPhN_2^+$ concentration to 9 μM. Therefore, the optimal concentration of $BrPhN_2^+$ was 5 μM.

Analytical Performance. Under the optimized conditions, the analytical performance of the eRAFT-polymerization-based biosensor was interrogated. As shown in Figure 3A, the sensing signal increases with the increase of the concentration of tDNA fragments. Thus, it is a "signal-on" biosensor, being insusceptible to the false-positive results.[12,18] As observed from Figure 3B, the sensing signal at ~0.3 V is logarithmically related to the concentration of tDNA fragment over 7 orders of magnitude spanning from 10 aM to 10 pM. The regression equation can be expressed as I (μA) = 4.01 + 1.31 log[C_{tDNA}/fM] (R^2 = 0.998). According to the $3\sigma_c$/slope criteria (σ_c represents the standard deviation of the control), the LOD is calculated to be 4.1 aM, which is lower than and/or comparable to those of other polymer-based electrochemical DNA biosensors, as summarized in Table 1. Compared with the previous eATRP-based biosensor,[18] for example, the LOD is downregulated by a factor of ~17.6, which is due to the introduction of many more Fc tags by the eRAFT polymerization. Although the LOD is comparable to that of the thermally initiated RAFT polymerization-based biosensor,[12] the eRAFT polymerization can be operated under fairly mild temperatures, which is impressive with respect to the detection of thermolabile biological molecules, such as nucleic acids and enzymes.

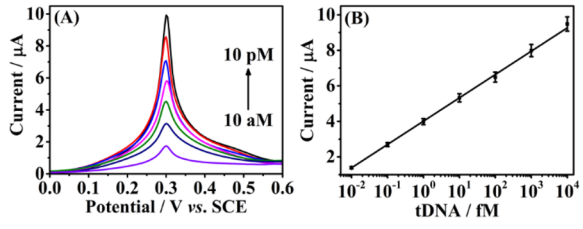

Figure 3. (A) SWVs corresponding to various concentrations of tDNA fragment over the range from 10 aM to 10 pM. (B) Calibration plot of the sensing signal at ~0.3 V against the logarithm of the concentration of the tDNA fragment. Error bars correspond to the standard deviations of five independent tests.

Reproducibility, Selectivity, Storage Stability, and Anti-interference Capability. The sensing reproducibility was tested by the intra-assays and interassays. Each test was fulfilled with five identically modified AuEs (with 10 pM tDNA fragment as the target). Of the intra-assay, the coefficient of variation is 4.3%, whereas of the interassay it is 4.7%. Thus, the sensing of tDNA fragments with the eRAFT-polymerization-based biosensor is reproducible.

The selectivity was tested using four different oligonucleotide fragments at the concentration of 10 pM. As shown in Figure 4A, all these mismatched oligonucleotide fragments can be effectively discriminated from the perfectly matched one (tDNA). Specifically, the presence of a single-base mismatch (SBM) or three-base mismatches (TBMs) causes a decrease of the sensing signal by about 72.6% or 84.8%; for the control fragment (cDNA), the sensing signal is almost the same as that of the background value. In view of its superb discrimination capability toward a SBM, the eRAFT-polymerization-based biosensor is applicable to the genotyping of SNPs.

The storage stability of the described electrochemical DNA biosensor was tested using two sets of identically modified electrodes. Each set was composed of five electrodes. One set was measured after the modification, and the other set was stored in a 4 °C refrigerator. After a fortnight storage, the sensing signal of the stored set at ~0.3 V is about 95.7% of that without storage. With this in mind, the storage stability of the eRAFT-polymerization-based biosensor is satisfactory.

Last, the anti-interference capability was challenged using 10% normal human serum (NHS) as the simulated matrix. The final concentrations of tDNA fragment in serum samples were 10 pM, 10 fM, and 10 aM, respectively. As can be seen from Figure 4B, the sensing signals at ~0.3 V from the matrices are 95.9% (10 pM), 91.7% (10 fM), and 86.2% (10 aM) of those from the serum-free samples, respectively. Thus, the eRAFT-polymerization-based biosensor features an acceptable anti-interference capability.

CONCLUSIONS

In summary, we have described an ultrasensitive and highly selective electrochemical DNA biosensor, by exploiting the eRAFT polymerization as a signal amplification strategy and the neutral oligonucleotide analogue PNA as the recognition element. Benefiting from the superb specificity of the PNA probe, the eRAFT polymerization-based biosensor is highly selective toward even a SBM. Through the eRAFT polymerization, a very large number of electroactive tags can be recruited, causing a substantial improvement of the sensing sensitivity. As a result, the combined use of the eRAFT

DOI: 10.1021/acssensors.8b01357
ACS Sens. XXXX, XXX, XXX−XXX

Table 1. Comparison of the Analytical Performance with Those of Other Polymer-Based Electrochemical DNA Biosensors

amplification strategy	grafting to/from	grafting temp	linear range	detection limit	refs
polythiophene	to	r.t.[a]	1.0 nM to 1.0 μM	0.5 nM	13
RCA	from	37 °C	10 aM to 10 pM	11 aM	20
TdT	from	37 °C	0.1 pM to 1.0 nM	20 fM	21
HCA	from	r.t.	1.0 fM to 1.0 pM	0.4 fM	23
SSHR	from	not provided	0.1 pM to 0.1 μM	0.1 pM	24
AGET ATRP	from	not provided	10.1 nM to .0 μM	15 pM	25
eATRP	from	r.t.	0.1 fM to 0.1 nM	72 aM	18
RAFT polymerization	from	47 °C	10 aM to 10 pM	3.2 aM	12
eRAFT polymerization	from	r.t.	10 aM to 10 pM	4.1 aM	this work

[a]room temperature.

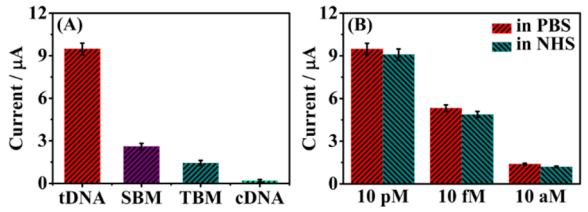

Figure 4. (A) Sensing signals at ~0.3 V corresponding to the four different oligonucleotide fragments at the concentration of 10 pM. (B) Sensing signals at ~0.3 V in the absence or presence of 10% serum. Error bars correspond to the standard deviations of five independent tests.

polymerization as a signal amplification strategy and the PNA probes as the recognition elements endows the described electrochemical DNA biosensor with high sensitivity and selectivity. Considering its high efficiency, easy operation, and low cost, this electrochemical DNA biosensor shows great promise in real applications. The eRAFT polymerization is taken advantage of as a signal amplification strategy for the first time in the electrochemical DNA biosensing. The eRAFT-polymerization-based strategy holds the following four advantages. First, the grafting of polymers based on the eRAFT polymerization is highly efficient. Second, relative to the strategies using dNTPs or oligonucleotide fragments as the monomers, it is low cost and shows a very low background signal. Third, compared with the ATRP-based strategies, it avoids the use of toxic transition metal complexes, which makes it biological friendly. Last, superior to the thermally initiated RAFT polymerization, it is applicable to the ultrasensitive detection of thermolabile biological molecules. Therefore, the eRAFT polymerization is very impressive as a signal amplification strategy.

■ ASSOCIATED CONTENT

Supporting Information

The Supporting Information is available free of charge on the ACS Publications website at DOI: 10.1021/acssensors.8b01357.

Figures including (1) a typical *i*−*t* curve of the eRAFT polymerization, (2) elemental mapping of the as-modified electrode, and (3) effect of $BrPhN_2^+$ concentration on the sensing signal and table listing probe and fragment sequences (PDF)

■ AUTHOR INFORMATION

Corresponding Authors

*(J.K.) E-mail: j.kong@njust.edu.cn. Tel.: +86-25-84303109.

*(L.N.) E-mail: lniu@gzhu.edu.cn. Tel.: +86-20-39366902.

*(X.Z.) E-mail: zhangxueji@ustb.edu.cn.

Notes

The authors declare no competing financial interest.

■ ACKNOWLEDGMENTS

This work was supported by the Project Funded by China Postdoctoral Science Foundation (Grant No. 2018M643040) and the National Natural Science Foundation of China (Grant No. 21575066).

■ REFERENCES

(1) Das, J.; Ivanov, I.; Montermini, L.; Rak, J.; Sargent, E. H.; Kelley, S. O. An electrochemical clamp assay for direct, rapid analysis of circulating nucleic acids in serum. *Nat. Chem.* **2015**, *7*, 569−575.

(2) Kaastrup, K.; Sikes, H. D. Polymerization-based signal amplification under ambient conditions with thirty-five second reaction times. *Lab Chip* **2012**, *12*, 4055−4058.

(3) Kou, B.; Chai, Y.; Yuan, Y.; Yuan, R. Dynamical regulation of enzyme cascade amplification by a regenerated DNA nanotweezer for ultrasensitive electrochemical DNA detection. *Anal. Chem.* **2018**, *90*, 10701−10706.

(4) Liu, Y.; Wei, M.; Liu, X.; Wei, W.; Zhao, H.; Zhang, Y.; Liu, S. Label-free ultrasensitive detection of telomerase activity via multiple telomeric hemin/G-quadruplex triggered polyaniline deposition and a DNA tetrahedron-structure regulated signal. *Chem. Commun.* **2016**, *52*, 1796−1799.

(5) Wang, G.; Das, J.; Ahmed, S.; Nemr, C. R.; Zhang, L.; Poudineh, M.; Sargent, E. H.; Kelley, S. O. Curvature-mediated surface accessibility enables ultrasensitive electrochemical human methyltransferase analysis. *ACS Sens.* **2018**, *3*, 1765−1772.

(6) Chuah, K.; Lai, L. M.; Goon, I. Y.; Parker, S. G.; Amal, R.; Gooding, J. J. Ultrasensitive electrochemical detection of prostate-specific antigen (PSA) using gold-coated magnetic nanoparticles as 'dispersible electrodes'. *Chem. Commun.* **2012**, *48*, 3503−3505.

(7) Liu, S.; Lin, Y.; Wang, L.; Liu, T.; Cheng, C.; Wei, W.; Tang, B. Exonuclease III-aided autocatalytic DNA biosensing platform for immobilization-free and ultrasensitive electrochemical detection of nucleic acid and protein. *Anal. Chem.* **2014**, *86*, 4008−4015.

(8) Ling, P.; Lei, J.; Ju, H. Porphyrinic metal-organic framework as electrochemical probe for DNA sensing via triple-helix molecular switch. *Biosens. Bioelectron.* **2015**, *71*, 373−379.

(9) Kwon, S. J.; Bard, A. J. DNA analysis by application of Pt nanoparticle electrochemical amplification with single label response. *J. Am. Chem. Soc.* **2012**, *134*, 10777−10779.

(10) Rasheed, P. A.; Sandhyarani, N. Electrochemical DNA sensors based on the use of gold nanoparticles: a review on recent developments. *Microchim. Acta* **2017**, *184*, 981−1000.

(11) Hu, Q.; Hu, W.; Kong, J.; Zhang, X. PNA-based DNA assay with attomolar detection limit based on polygalacturonic acid mediated in-situ deposition of metallic silver on a gold electrode. *Microchim. Acta* **2015**, *182*, 427−434.

DOI: 10.1021/acssensors.8b01357
ACS Sens. XXXX, XXX, XXX−XXX

(12) Hu, Q.; Han, D.; Gan, S.; Bao, Y.; Niu, L. Surface-initiated-reversible-addition−fragmentation-chain-transfer polymerization for electrochemical DNA biosensing. *Anal. Chem.* **2018**, *90*, 12207−12213.
(13) Le Floch, F.; Ho, H. A.; Harding-Lepage, P.; Bedard, M.; Neagu-Plesu, R.; Leclerc, M. Ferrocene-functionalized cationic polythiophene for the label-free electrochemical detection of DNA. *Adv. Mater.* **2005**, *17*, 1251−1254.
(14) Wu, Y.; Liu, S.; He, L. Polymerization-assisted signal amplification for electrochemical detection of biomarkers. *Analyst* **2011**, *136*, 2558−2563.
(15) Yuan, L.; Wei, W.; Liu, S. Label-free electrochemical immunosensors based on surface-initiated atom radical polymerization. *Biosens. Bioelectron.* **2012**, *38*, 79−85.
(16) Gibbs, J. M.; Park, S. J.; Anderson, D. R.; Watson, K. J.; Mirkin, C. A.; Nguyen, S. T. Polymer-DNA hybrids as electrochemical probes for the detection of DNA. *J. Am. Chem. Soc.* **2005**, *127*, 1170−1178.
(17) Baskaran, D.; Mays, J. W.; Bratcher, M. S. Polymer-grafted multiwalled carbon nanotubes through surface-initiated polymerization. *Angew. Chem.* **2004**, *116*, 2190−2194.
(18) Hu, Q.; Wang, Q.; Sun, G.; Kong, J.; Zhang, X. Electrochemically mediated surface-initiated de novo growth of polymers for amplified electrochemical detection of DNA. *Anal. Chem.* **2017**, *89*, 9253−9259.
(19) Hu, Q.; Wang, Q.; Jiang, C.; Zhang, J.; Kong, J.; Zhang, X. Electrochemically mediated polymerization for highly sensitive detection of protein kinase activity. *Biosens. Bioelectron.* **2018**, *110*, 52−57.
(20) Ji, H.; Yan, F.; Lei, J.; Ju, H. Ultrasensitive electrochemical detection of nucleic acids by template enhanced hybridization followed with rolling circle amplification. *Anal. Chem.* **2012**, *84*, 7166−7171.
(21) Yang, F.; Yang, X.; Wang, Y.; Qin, Y.; Liu, X.; Yan, X.; Zou, K.; Ning, Y.; Zhang, G. J. Template-independent, in situ grown DNA nanotail enabling label-free femtomolar chronocoulometric detection of nucleic acids. *Anal. Chem.* **2014**, *86*, 11905−11912.
(22) Hun, X.; Xie, G.; Luo, X. Scaling up an electrochemical signal with a catalytic hairpin assembly coupling nanocatalyst label for DNA detection. *Chem. Commun.* **2015**, *51*, 7100−7103.
(23) Jia, L.; Shi, S.; Ma, R.; Jia, W.; Wang, H. Highly sensitive electrochemical biosensor based on nonlinear hybridization chain reaction for DNA detection. *Biosens. Bioelectron.* **2016**, *80*, 392−397.
(24) Xia, F.; White, R. J.; Zuo, X.; Patterson, A.; Xiao, Y.; Kang, D.; Gong, X.; Plaxco, K. W.; Heeger, A. J. An electrochemical supersandwich assay for sensitive and selective DNA detection in complex matrices. *J. Am. Chem. Soc.* **2010**, *132*, 14346−14348.
(25) Wu, Y.; Liu, S.; He, L. Electrochemical biosensing using amplification-by-polymerization. *Anal. Chem.* **2009**, *81*, 7015−7021.
(26) Lou, X.; Lewis, M. S.; Gorman, C. B.; He, L. Detection of DNA point mutation by atom transfer radical polymerization. *Anal. Chem.* **2005**, *77*, 4698−4705.
(27) Wang, J. S.; Matyjaszewski, K. Controlled/"living" radical polymerization. Atom transfer radical polymerization in the presence of transition-metal complexes. *J. Am. Chem. Soc.* **1995**, *117*, 5614−5615.
(28) He, P.; Zheng, W.; Tucker, E. Z.; Gorman, C. B.; He, L. Reversible addition−fragmentation chain transfer polymerization in DNA biosensing. *Anal. Chem.* **2008**, *80*, 3633−3639.
(29) Chiefari, J.; Chong, Y. K.; Ercole, F.; Krstina, J.; Jeffery, J.; Le, T. P. T.; Mayadunne, R. T. A.; Meijs, G. F.; Moad, C. L.; Moad, G.; Rizzardo, E.; Thang, S. H. Living free-radical polymerization by reversible addition−fragmentation chain transfer: the RAFT process. *Macromolecules* **1998**, *31*, 5559−5562.
(30) Destarac, M.; Charmot, D.; Franck, X.; Zard, S. Z. Dithiocarbamates as universal reversible addition-fragmentation chain transfer agents. *Macromol. Rapid Commun.* **2000**, *21*, 1035−1039.
(31) Perrier, S. 50th Anniversary perspective: RAFT polymerization—a user guide. *Macromolecules* **2017**, *50*, 7433−7447.
(32) Tian, X.; Ding, J.; Zhang, B.; Qiu, F.; Zhuang, X.; Chen, Y. Recent advances in RAFT polymerization: Novel initiation mechanisms and optoelectronic applications. *Polymers* **2018**, *10*, 318.
(33) Hill, M. R.; Carmean, R. N.; Sumerlin, B. S. Expanding the scope of RAFT polymerization: Recent advances and new horizons. *Macromolecules* **2015**, *48*, 5459−5469.
(34) Moad, G.; Chiefari, J.; Krstina, J.; Mayadunne, R. T. A.; Postma, A.; Rizzardo, E.; Thang, S. H.; Chong, B. Y. K. Living free radical polymerization with reversible addition−fragmentation chain transfer (the life of RAFT). *Polym. Int.* **2000**, *49*, 993−1001.
(35) Boyer, C.; Bulmus, V.; Davis, T. P.; Ladmiral, V.; Liu, J.; Perrier, S. Bioapplications of RAFT polymerization. *Chem. Rev.* **2009**, *109*, 5402−5436.
(36) Moad, G. RAFT polymerization to form stimuli-responsive polymers. *Polym. Chem.* **2017**, *8*, 177−219.
(37) Baussard, J. F.; Habib-Jiwan, J. L.; Laschewsky, A.; Mertoglu, M.; Storsberg, J. New chain transfer agents for reversible addition-fragmentation chain transfer (RAFT) polymerisation in aqueous solution. *Polymer* **2004**, *45*, 3615−3626.
(38) Wang, Y.; Fantin, M.; Park, S.; Gottlieb, E.; Fu, L.; Matyjaszewski, K. Electrochemically mediated reversible addition−fragmentation chain-transfer polymerization. *Macromolecules* **2017**, *50*, 7872−7879.
(39) Egholm, M.; Buchardt, O.; Nielsen, P. E.; Berg, R. H. Peptide nucleic acids (PNA). Oligonucleotide analogs with an achiral peptide backbone. *J. Am. Chem. Soc.* **1992**, *114*, 1895−1897.
(40) Nielsen, P. E.; Egholm, M.; Berg, R. H.; Buchardt, O. Sequence-selective recognition of DNA by strand displacement with a thymine-substituted polyamide. *Science* **1991**, *254*, 1497−1500.
(41) Das, J.; Ivanov, I.; Sargent, E. H.; Kelley, S. O. DNA clutch probes for circulating tumor DNA analysis. *J. Am. Chem. Soc.* **2016**, *138*, 11009−11016.
(42) Wipawakarn, P.; Ju, H.; Wong, D. K. A label-free electrochemical DNA biosensor based on a Zr(IV)-coordinated DNA duplex immobilised on a carbon nanofibre|chitosan layer. *Anal. Bioanal. Chem.* **2012**, *402*, 2817−2826.
(43) Allongue, P.; Delamar, M.; Desbat, B.; Fagebaume, O.; Hitmi, R.; Pinson, J.; Savéant, J. M. Covalent modification of carbon surfaces by aryl radicals generated from the electrochemical reduction of diazonium salts. *J. Am. Chem. Soc.* **1997**, *119*, 201−207.
(44) Barner-Kowollik, C.; Davis, T. P.; Stenzel, M. H. Synthesis of star polymers using RAFT polymerization: what is possible? *Aust. J. Chem.* **2006**, *59*, 719−727.
(45) Stenzel, M. H.; Zhang, L.; Huck, W. T. Temperature-responsive glycopolymer brushes synthesized via RAFT polymerization using the Z-group approach. *Macromol. Rapid Commun.* **2006**, *27*, 1121−1126.
(46) Duréault, A.; Taton, D.; Destarac, M.; Leising, F.; Gnanou, Y. Synthesis of multifunctional dithioesters using tetraphosphorus decasulfide and their behavior as RAFT agents. *Macromolecules* **2004**, *37*, 5513−5519.
(47) Magenau, A. J.; Strandwitz, N. C.; Gennaro, A.; Matyjaszewski, K. Electrochemically mediated atom transfer radical polymerization. *Science* **2011**, *332*, 81−84.

DOI: 10.1021/acssensors.8b01357
ACS Sens. XXXX, XXX, XXX−XXX